

Local Structural Probes around High-Z Elements in a Solid: EXAFS vs. EXELFS

F.M. Alamgir, H. Jain, and D.B. Williams,

Dept. Materials Science and Engineering, Lehigh University, Bethlehem, PA

Extended x-ray absorption fine structure (EXAFS) analysis is one of the most commonly used methods for determining local structure of solids. It is element specific and therefore, even complex multi-component structures can be determined, if the information around all the elements is accessible. There are, however, significant limitations of the conventional EXAFS. To begin with, accessing the K-edges below 3 keV becomes problematic since absorption at these energies requires sub-micron sample thickness for transmission EXAFS and very few beamlines are available to do fluorescence EXAFS. Also, the spatial resolution of X-rays is not high enough to study sub-micron scale phases.

The electron analogue of EXAFS is the extended electron energy loss fine structure (EXELFS) within electron energy-loss spectroscopy (EELS) in a transmission electron microscope (TEM). Downstream from a sample in a TEM, the Parallel Electron Energy-Loss Spectrometer (PEELS) provides a unique capability of acquiring information on the atomic structure. As the synchrotron X-rays do in EXAFS, the incident electron beam in a TEM ionizes an atom and the resulting ejected electrons occupy energy levels in the conduction band of the sample. These modulations appear as oscillations beyond the ionization edge in an EELS or an X-ray absorption spectrum. Both of these types of oscillations are represented as a function $\chi(\mathbf{k})$, where \mathbf{k} is the momentum transferred to the ionized electrons. The Fourier transform of $\chi(\mathbf{k})$, $\text{FT}[\chi(\mathbf{k})]$, is proportional to the radial distribution function (RDF), which represents the probability of finding an atom at a given radial distance from the ionized atom. Since the incident electrons in a TEM can be focused with magnetic lenses, EXELFS offers the unique ability to obtain atomic and electronic structure on a nanometer-scale spatial resolution. Further, since TEMs operate in high vacuum and use thin specimens, EELS is especially suited to K-edge analysis of low atomic number elements.

Because the probability of an ionization event in EELS decreases rapidly as the ionization energy approaches the energy of the incident electrons, the K-edges of elements of atomic number > 24 become very difficult to access using detectors currently available¹. For these elements, EXELFS is restricted to the analysis of the complicated but accessible L-edges where the fine structure is a convolution of structure from elec-

trons of several different L transitions. For even higher atomic number elements, we reach K-edge transition energies for which most EXAFS beamlines are not optimized, and so, even for EXAFS one must resort to these lower energy, but complicated L-edges. We have attempted to establish a methodology for the treatment of L-edges by performing a comparative study between the L-edge EXELFS and K-edge EXAFS of a standard system, fcc nickel. The results also provide the first direct comparison of the advantages and disadvantages of these two techniques.

TEM samples of Ni were prepared from 99.9% pure foils by mechanically thinning and ion-polishing down to a thickness of 50 nm. A Philips EM400 120 keV TEM with a PEELS system was used for acquiring Ni EEL spectra. Channel to channel variations in the gain of the photodiodes were removed by averaging the 8 different EELS spectra using different sets of photodiode channels. K-edge EXAFS of a 12 μm thick Ni foil, same as that used to prepare TEM specimens, was measured in transmission at the X23A2 beamline of the National Synchrotron Light Source (NSLS). For EXELFS, the dark-current noise, and the pre-edge background were removed from raw EEL spectra by using a simple power-law function. The contribution of plural scattering was removed by applying the Fourier-ratio deconvolution².

The EXAFS and EXELFS data were processed using the WinXAS 97 software³, giving the function $\chi(\mathbf{k})\mathbf{k}^n$, with \mathbf{k}^n weighting factor to correct for the decaying of the amplitude. The reduction of the energy loss function from the L-edge in EXELFS to the final $\text{FT}[\chi'(\mathbf{k})]$ involves first the isolation of the L_3 contribution to the energy-loss function and second, a weighting of the extracted $\chi(\mathbf{k})$ by a factor that adjusts for the relatively stronger decay of the EXELFS amplitude with respect to that of EXAFS. After this point, the data are processed in the same way as for EXAFS described above. Briefly, the L_1 -edge is first removed using a step function with the assumption that the contribution of L_1 electrons to the total fine structure is negligible⁴. A step function is used with a 5th order polynomial fit to the background before and after the step (figure 1a, dotted line to dashed line). Next, the L_3 and L_2 contributions are separated based on a simple assumption that the information carried by these two electrons is identical, but weighted by their respective photo-ionization cross-

sections and shifted by the spin-orbit splitting energy ($\Delta=17$ eV for Ni). Details of this procedure have been published elsewhere⁵. The solid red plot in figure 1 is the result of removing the L_2 and L_1 contributions, and we see that this eliminates completely the artifact peak that we observe at an unphysical distance of 1 Å in the RDF in figure 1c.

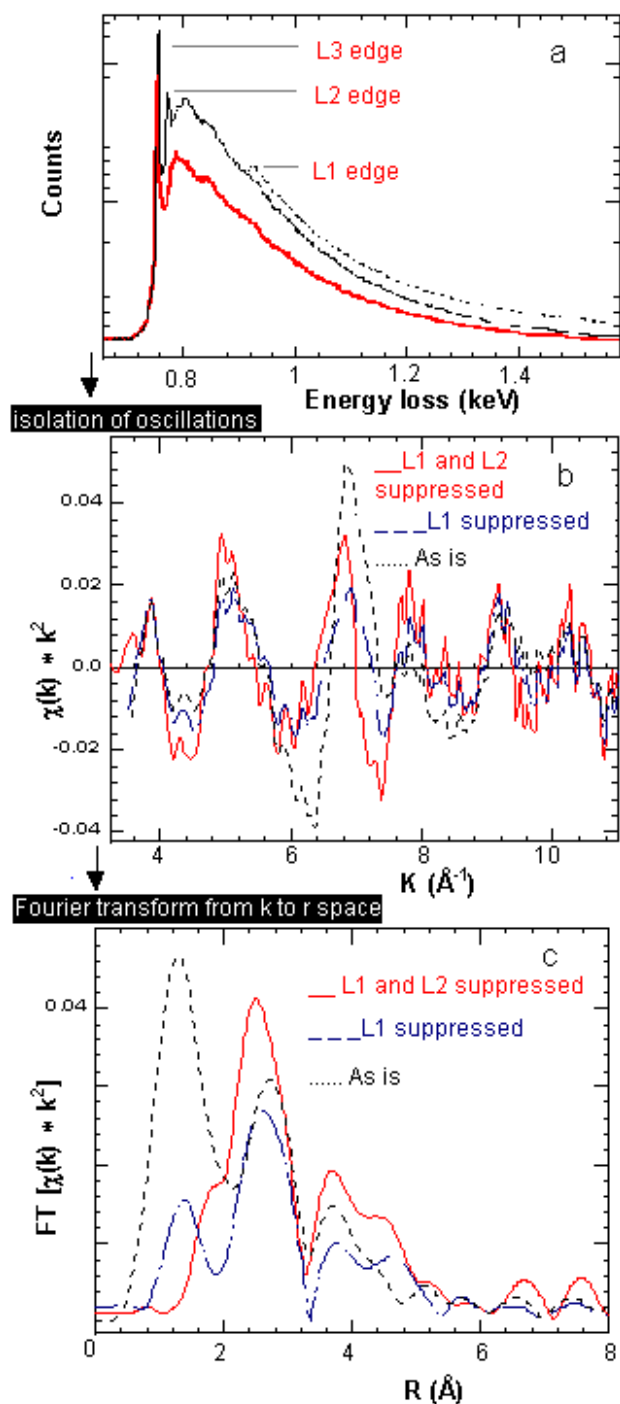


Figure 1. (a) The removal of the L_1 step and the L_2 contribution from the Ni L-edge, (b) the effect of this processing on the $\chi(k)$ and (c) the effect on $\text{FT}[\chi(k)]$.

The structural information in both EXELFS and EXAFS arises from ionized electrons as they sample the neighboring atomic potentials. However, since the incident radiation is different in the two cases, there are some differences to consider between them. In the limit of small momentum transfer from the incident electron to the sample in EELS, the ratio of the signal counting rates for EXELFS and EXAFS, Γ_e and Γ_{ph} respectively, is given by⁶:

$$\frac{\Gamma_e}{\Gamma_{ph}} = \xi \frac{\ln[1 + \mathbf{q}_0^2 / \mathbf{q}^2]}{\hbar \omega} \quad (1)$$

where, \mathbf{q}_0 is the transverse momentum resolution of the spectrometer in EELS, \mathbf{q} is the scattering vector of the inelastically scattered electron in EELS, ω is the frequency of the ionized electron waves and ξ is a constant that depends on the instrumental conditions and

the sample thickness. Since $\hbar \omega$ increases faster than the log factor, the EXELFS signal exhibits an overall decrease in amplitude with increasing energy in comparison to that of EXAFS. Direct comparison between EXELFS and EXAFS requires a re-normalization of the amplitudes of the oscillations using equation (1)⁷, thus modifying $\chi(\mathbf{k})$ to $\chi'(\mathbf{k})$ for EXELFS.

The useful k-range of EXAFS extends to about 15.5\AA^{-1} whereas in EXELFS this range extends only to 11\AA^{-1} (figure 2) and so we have plotted $\text{FT}_{\text{EXAFS}}[\chi'(\mathbf{k})]$ for both the full range and the limited range of EXELFS. The comparison between $\text{FT}[\chi'(\mathbf{k})]$ of Ni L_3 and Ni K as obtained from EXELFS and EXAFS, respectively, is shown in figure 2. We note in figure 3 that the full-width-at-half-maximum of the nearest neighbor (nn) peak matches well for EXELFS and EXAFS when using the same k-range. On this figure the peaks labeled nn2, nn3 and nn4 refer to the 2nd, 3rd and 4th nearest neighbors, corresponding to $\sqrt{2}$ -, $\sqrt{3}$ - and 2-times the nearest neighbor distance, respectively. The position of the 2nd nn peak (nn2) is more pronounced in Ni EXELFS than in EXAFS. We believe that this is due, in part, to the difference in the final state wavefunctions of the electrons after L_3 and K transitions, respectively. That is, the d-type electrons of the L_3 transition in fcc Ni “see” the atomic neighbors slightly differently than do the p-type electrons in a K transition.

The radial probability density of the 4d final-state wavefunction of L-transitions in such metals goes to zero from 4 to 6 Å⁸. On the other hand, the radial probability density of the 3p final-state wavefunction of K-transitions has a maximum over the same radial range. Hence, beyond the 2nd nn peak the information in L-edge EXELFS is very strongly damped, whereas in K-edge EXAFS it is easy to probe as far as the 4th nn (figure 3).

Finally, the effects of sample damage due to the beam can be different in EXAFS and EXELFS experiments. The potential for structural change from the radiation dosage to the sample is not a problem in EXAFS since only about 10^{-8} photons are absorbed per atom per second⁹, whereas for high resolution EXELFS the dosage per atom per second is about 10^2 electrons, 10 orders of magnitude higher⁹. This could lead to problems in a material with poor electrical and thermal conduction. For metals, however, the primary cause for sample damage is the direct impact of incident electrons¹⁰, but for Ni we did not observe any sample damage due to the beam in our experiments.

To summarize our findings, a methodology for the analysis of L-edges in EXELFS has been established. A comparison of EXELFS from fcc Ni L-edge with those of EXAFS from the K-edge of the same sample shows that the 1st and 2nd nearest-neighbor distances match well in the two techniques. A scheme is proposed for isolating the L_3 contribution to the fine structure beyond the L-edge. Our findings indicate that the EXELFS of L-edges provides information to at least the 2nd coordination shell, whereas K-edge EXAFS, with much poorer spatial resolution, can provide structure to the 4th nearest neighbors.

Acknowledgements

This work is supported by the Basic Energy Sciences Division of the US Department of Energy (Grant no. DE-FG02-95ER45540). We would like to thank Slade Cargill III, Yasuo Ito and Joe Woicik for their help

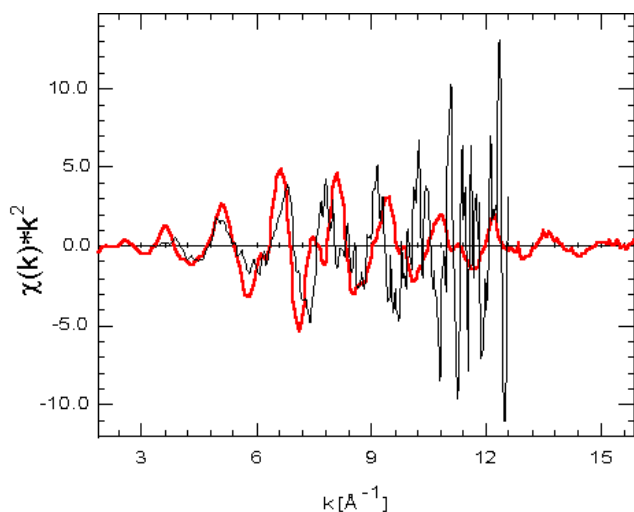


Figure 2. EXELFS oscillations (thin black line) and EXAFS oscillations (thick red line) for fcc Ni. Beyond the range of $3.5 < k < 11.5$ the noise dominates the EXELFS signal.

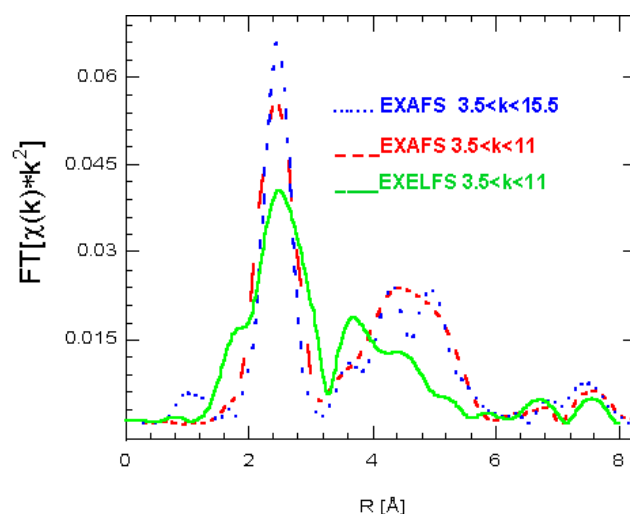


Figure 3. The $FT[\chi'(k)]$ using K-edge EXAFS and L-edge EXELFS are shown for Ni.

with the experiments. Research carried out (in whole or in part) at the National Synchrotron Light Source, Brookhaven National Laboratory, which is supported by the U.S. Department of Energy, Division of Materials Sciences and Division of Chemical Sciences, under Contract No. DE-AC02-98CH10886.

References

- [1] G. Hug, G. Blanche, M. Jaoyen, A.M. Flank and J. Rehr, *Ultramicroscopy*, **59**, 1995, 121.
- [2] R.F. Egerton, *Electron Energy-Loss Spectroscopy in the Electron Microscope*, 2nd edn. (New York: Plenum Press), 247, 1996.
- [3] T. Ressler, "WinXAS: a New Software Package Not Only for the Analysis of Energy-dispersive XAS Data", *J. de Phys.*, **7**, 269, 1997.
- [4] R.D. Leapman, L.A. Grunes, P.L. Fejes, and J. Silcox, 1981, *EXAFS Spectroscopy: Techniques and Applications*, edited by B.K. Teo, and D.C. Joy, New York: Plenum, 217.
- [5] F.M. Alamgir, Y. Ito, H. Jain, and D.B. Williams, *Phil. Mag. Lett.*, **81**, 3, 213, 2001.
- [6] B. M. Kincaid, A.E. Meixner, and P.M. Platzman, 1995, *Phys. Rev. Lett.*, **40**, 19, 1296.
- [7] M. Qian, M. Sarikaya, and E. Stern, "Development of the EXELFS technique for high accuracy structural information", 1995, *Ultramicroscopy*, **59**, 137, 1995.
- [8] R.A. Alberty, *Physical Chemistry*, 2nd edition, New York: Wiley, 343-345, 1997.
- [9] T.M. Hayes and J.B. Boyce, *EXAFS Spectroscopy*, Solid State Physics Advances in Research and Applications, New York: Academic Press, 173, 1982.
- [10] L.W. Hobbs, *Introduction to Analytical Electron Microscopy*, ed. J.J. Hren, J.I. Goldstein, and D.C. Joy, (New York: Plenum Press), 437, 1979.